Preconditioning of projected sirt algorithm for electromagnetic tomography

Jianna Hao[1], Wuliang Yin[2], Qian Zhao[1], Xu Kai[1], Guang Chen[1]

[1]School of Electrical Engineering and Automation
Tianjin University
Tianjin, China
Email: haojianna@gmail.com

[2]School of Electrical and Electronic Engineering
University of Manchester
M60 1QD, UK
Email: wuliang.yin@manchester.ac.uk

Abstract—**For Electromagnetic Tomography (EMT) Techniques, image reconstruction is one of the crucial steps, which directly affects the quality of reconstruction and real-time performance of the EMT system. Following analyzing a prior iteration method for SIRT (simultaneous iterative reconstruction technique) algorithm, a preconditioning for the projected SIRT is proposed to accelerate the image reconstruction speed and alleviate the ill-posed nature of the EMT inverse problem. Experimental tests confirm that the quality of the reconstructed images using the preconditioning algorithm is enhanced with only a small number of iterations required.**

Keywords-Electromagnetic Tomography; image reconstruction; preconditioning; projected SIRT

I. INTRODUCTION

Electromagnetic tomography technology, which is based on electromagnetic induction theory, is a relatively new modality of electrical tomography technique. Compared with other electrical tomography techniques (e.g. ERT and ECT), the unique advantage of EMT is its ability to derive both the electrical conductivity and magnetic permeability distribution [1]. Over the recent several decades, the EMT technology has drawn more and more attention of researchers in this field. The EMT technology can be used in many fields such as industrial multi-phase flow measurement [14], human detection and tomography and other applications where conductivity and permeability distributions are sought [2].

The EMT technology aims to reconstruct images of the object distribution. Therefore, developing effective image reconstruction algorithms is extremely urgent for its practical applications. In 1996, researchers in University of Averio first developed a 16-electrode EMT system, and the heuristic algorithm and ART algorithm were used for image reconstruction [3]. Afterwards, A.V. Korzhenevskii and others proposed back projection algorithm for image reconstruction [4]. In [5], the authors accounted and evaluated various image reconstruction algorithms in EMT such as LBP, Tikhonov Regularized algorithm, ART, SIRT, Newton-Raphson, Landweber algorithm and so on.

In general, image reconstruction algorithms for EMT can be divided into two groups, non-iterative algorithms and iterative algorithms. Because the non-linear relationship between the conductivity distribution and the voltage, it is almost impossible to find an accurate solution by any non-iterative algorithm based on a simplified linear model. To improve the image quality, the inverse problem has to be solved iteratively. Unfortunately, the iterative algorithms are usually very time-consuming. In this paper, the prior iteration online reconstruction method was applied in the SIRT algorithm for the first time to ensure the real-time performance of image reconstruction for EMT. Moreover, in order to further improve the convergence rate and stabilize the solution, the projected SIRT algorithm together with its preconditioning version were proposed to increase the image quality, and experimental tests discussed below confirmed that a few iteration steps of preconditioning projected SIRT was suitable for online reconstruction meanwhile.

II. EMT IMAGE RECONSTRUCTION MODEL

Similar to other electrical tomography techniques, EMT involves the forward problem and inverse problem. The inverse problem of the EMT system mainly includes the designing and implement of image reconstruction algorithm [6], which is a crucial part of the EMT technology.

Assuming a linear forward model, the image reconstruction can be simplified as follows:

$$z = Sg \tag{1}$$

where z is an $m \times 1$ dimensional vector indicating the voltage values. g is an $n \times 1$ dimensional vector standing for the conductivity distribution, and it denotes the gray level values in the reconstructed images. S is a sensitivity matrix of dimension $m \times n$. The sensitivity matrix can be mainly derived from the following methods: 1) semi-analysis method [7]; 2) finite element model simulation method [8]; 3) experimental method [9]. As a result of that the sensitivity matrix from the experimental method is closest to the practical EMT system, the sensitivity matrix is obtained by this method in this paper.

The task of EMT inverse problem is solving g in (1) rapidly and efficiently from known S and z. There are two major difficulties associated with (1). Firstly, it is under-determined due to the number of unknown variables n is usually much larger than the number of the measurement values m. Therefore, the solution is not unique. Secondly, (1) is ill conditioned, which means that the solution of (1) is sensitive to small perturbations of z. SIRT algorithm is

adopted here due to its advantage of being able to control noise effectively.

III. SIRT ALGORITHM

A. SIRT Algorithm

The SIRT algorithm is commonly used for image reconstruction in x-ray computerized tomography. Recently, SIRT has been used in EMT. The SIRT algorithm can be formulated as follows:

$$g_{k+1} = g_k - \alpha_k S^T \frac{Sg_k - z}{diag(SS^T)} \qquad (2)$$

where the initial value of g is derived from the LBP method, i.e., $g_0 = S^T z$, α_k is a relaxation factor, $diag(SS^T)$ is a vector composed of diagonal components of SS^T and the division means that each numerator is divided by the corresponding denominator. For the purpose of mathematical analysis more conveniently, (2) is equivalent to the following equation

$$g_{k+1} = g_k - \alpha_k S^T W(Sg_k - z) \qquad (3)$$

where $W \in R^{m \times m}$ is a diagonal matrix with each component on the diagonal denotes as the reciprocal of responding component of $Q = diag(SS^T)$, that is $W(i,i) = 1/Q(i,1)$, here, W can be seen as a weighting matrix.

B. Projected SIRT

A critical drawback for SIRT is that it usually requires a large number of iterations and hence its convergence characteristic is poor. It has been found that inclusion of the constraint function is necessary in order to regularize the iteration and to produce a stable solution [15]. As a result, a projected operator was introduced to improve its convergence quality, and it can be expressed by:

$$g_{k+1} = P\{g_k - \alpha_k S^T W(Sg_k - z)\} \qquad (4)$$

where

$$P[f(x)] = \begin{cases} 0, & if \quad f(x) < 0 \\ f(x), & if \ 0 \le f(x) \le 1 \\ 1, & if \quad f(x) > 1 \end{cases} \qquad (5)$$

Although the projected SIRT method can improve the convergence quality to some extent, it still needs a lot of iterations to provide a satisfactory approximation of the true object distribution, so this method is not suitable for real-time reconstruction. Therefore, a preconditioning is applied to the projected SIRT algorithm to accelerate the convergence in this work:

$$g_{k+1} = P\{g_k - \beta Y S^T W(Sg_k - z)\} \quad (k = 0,1,2,3,\ldots M) \qquad (6)$$

where Y is a preconditioned matrix, β is a relaxation factor, and $g_0 = S^T z$.

In the following section, we will discuss how to choose the preconditioned matrix. Before that, a prior iterative version of (3) is proposed, this prior iteration method not only realized the online image reconstruction, but also deduced how to derive the preconditioned matrix.

C. Prior iteration for SIRT

In [11], a prior iteration method is proposed to realize the online image reconstruction, and it has proved the following two sets of equations are equivalent.

$$x_{k+1} = A_k x_k + B_k v \qquad (k = 0,1,2,3,\ldots) \qquad (7)$$

$$\begin{cases} D_{k+1} = A_k D_k + B_k \\ x_{k+1} = D_{k+1} v \end{cases} \qquad (k = 0,1,2,3,\ldots) \qquad (8)$$

where A_k, B_k and D_k are three generic matrixes. $A_k \in R^{n \times n}$, $B_k \in R^{n \times m}$ and $D_k \in R^{n \times m}$, and v is a generic vector $v \in R^m$.

This iterative method was used in Landweber algorithm in [11]. In this paper, we applied it to the SIRT algorithm for EMT image reconstruction, (3) can be rearranged as:

$$g_{k+1} = g_k + \alpha_k S^T W z - \alpha_k S^T W S g_k$$
$$= (I_n - \alpha_k S^T W S) g_k + \alpha_k S^T W z \qquad (9)$$

Let $I_n - \alpha_k S^T WS = A_k$, $\alpha_k S^T W = B_k$, then

$$g_{k+1} = A_k g_k + B_k z \qquad (10)$$

By contrasting with (7) and (8), let $x_k = g_k$ and $v = z$, then (10) is equivalent to

$$D_{k+1} = A_k D_k + B_k = (I_n - \alpha_k S^T WS)D_k + \alpha_k S^T W \qquad (11)$$

$$g_k = D_k z \qquad (12)$$

where $D_0 = S^T$. Actually, D_k can be seen as the approximate of generalized inverse of S, and it is iterated a few times to generate a matrix D_N. Plugging D_N into (12), then an image can be reconstructed in the same way as LBP.

The parameter α_k is derived by minimizing the norm of the error vector in each step of the iteration process through the following procedure:

$$e_k = z - Sg_k \qquad (13)$$

$$e_{k+1} = z - Sg_{k+1} = z - S(g_k - \alpha_k S^T W(Sg_k - z))$$
$$= e_k - \alpha_k SS^T W e_k \qquad (14)$$

Let $f_k = \|e_k\|_2^2$, then

$$f_{k+1} = \|e_{k+1}\|_2^2 = \|e_k - \alpha_k SS^T W e_k\|_2^2 \qquad (15)$$

The objective is to minimize f_{k+1} at each step by letting

$$\frac{df_{k+1}}{d\alpha_k} = 0 \qquad (16)$$

Solving this equation, α_k is found to be

$$\alpha_k = \frac{e_k^T SS^T We_k}{\left\| SS^T We_k \right\|_2^2} \qquad (17)$$

As it has been mentioned in [11], a measurement vector z only influences the step-length, a different z should result in almost the same D_N if it is converged through a sufficient number of iterations. For the purpose of offline iteration conveniently, z is denoted as z_0 with all the components are 1 when calculate α_k. Only the number of iteration steps N is undetermined due to the optimal length is adopted.

In conclusion, the prior iteration online reconstruction algorithm (we named it PIOR for short) for SIRT algorithm can be summarized as follows:

$$\begin{cases} a)\, e_k = z_0 - SD_k z_0 \\ b)\, \alpha_k = \dfrac{e_k^T SS^T We_k}{\left\| SS^T We_k \right\|_2^2} \qquad (k=0,1,2,3,\ldots N) \\ c)\, D_{k+1} = (I_n - \alpha_k S^T WS)D_k + \alpha_k S^T W \end{cases} \qquad (18)$$

$$g = D_N z$$
(19)

Actually, D_N can be seen as the approximate of generalized inverse of S, and D_N is solved by variable step searching approach. Although the PIOR method can realize the prior iteration and online reconstruction, the quality of the image is not improved compared to the original SIRT algorithm (3), and it will be illustrated by the experimental tests below.

D. Acceleration of Projeted SIRT Algorithm

As it has been referred in [10], (2) can be deduced from the Landweber iteration by replacing the relaxation factor with a weighting matrix. In essence, SIRT is also a descent gradient method. Its principle is the same as that of Landweber iteration. In [12], the authors proposed that one of the choices of the preconditioning matrix for Landweber iteration algorithm is a polynomial function of $S^T S$. Similarly, for the SIRT algorithm, the preconditioning matrix Y is assumed as a polynomial function of $S^T WS$ here. According to the recursive method, equation c) in (18) is equivalent to the following expression:

$$\begin{cases} Y_{k+1} = Y_k + \alpha_k(I_n - S^T WSY_k) \qquad (k=0,1,2,\ldots N) \\ D_N = Y_N S^T W \end{cases} \qquad (20)$$

From (20), it is apparently that Y_N is the function of $S^T WS$, so Y_N can be a preconditioned matrix here. Due to the reason of convenient calculation, (18) is virtually adopted for preconditioning. Consequently, (6) is reformulated as follows:

$$g_{k+1} = P\{g_k - \beta D_N(Sg_k - z)\} \quad (k=0,1,2,3,\ldots M) \qquad (21)$$

where D_N is determined by (15), and the convergence condition is

$$0 < \beta < \frac{2}{\left\| D_N S \right\|_2}$$

As a result of the infliction of preconditioning matrix Y_N, the convergence rate of projected SIRT method is improved significantly, and this method is named as accelerated projected SIRT algorithm based on generalized inverse (noted as APSA for short). After a few iteration steps, the satisfactory reconstruction image can be derived.

IV. EXPERIMENTAL TESTS

In this section, experimental tests were carried out to validate the effectiveness of the methods developed in this paper.

An 8-coil sensor was chosen for the experiments [13]. The diameter of the object space is $15cm$. The images were presented on a 15×15 pixels digitized image. The algorithms were implemented in Matlab. Fig.1 shows the real distribution with the black standing for high conductive materials, and the white color denoting air.

A common issue with the descent gradient methods is that they can only guarantee converging to a local minimum. If the iteration process is not stopped after certain number of iterations, it is unlikely to derive a good image. It is difficult to decide that when and how the iterative process should be stopped. In this paper, the number of iterations of the SIRT and projected SIRT is chosen by empirically. For the SIRT and projected SIRT algorithms, the number of iterations is 1000 times and 200 times respectively, and the corresponding reconstructed images are shown in Fig.2 and Fig.3. From Fig.2 and Fig.3, it is easy to find that projected SIRT algorithms is not always better than original SIRT, (a) in Fig.3 is fairly distortional relative to the true distribution of Fig.1, and (b) in Fig.3 appeared serious artifacts in the reconstruction image.

It is proved by running a program that when $k \geq 80$, e_k in (18) stays almost the same value for the sensitivity matrix considered in this paper, that is, when $k \geq 80$, D_k converges to D_N ($N = 80$). Therefore, let $N = 80$ is enough for the algorithm PIOR and APSA. For APSA method, the relaxation factor $\beta = 1.9501$, this is the maximum value without divergence. In order to guarantee the real-time performance of online image reconstruction, PSGI is executed for 5 iterations, i.e. $M = 5$ in (21). Fig.4 and Fig.5 show the reconstructed results by the PIOR algorithm and APSA method respectively.

Two criteria, namely relative image error and correlation coefficient between the test object and reconstruction, were used to evaluate the method described in this work.

$$\text{Image error} = \frac{\left\| \hat{g} - g \right\|}{\left\| g \right\|} \qquad (22)$$

$$\text{Correlation coefficient} = \frac{\sum_{i=1}^n (\hat{g}_i - \bar{\hat{g}})(g_i - \bar{g})}{\sqrt{\sum_{i=1}^n (\hat{g}_i - \bar{\hat{g}})^2 \sum_{i=1}^n (g_i - \bar{g})^2}} \qquad (23)$$

where g is the true conductivity distribution of the test model, $\hat{g}$ is the reconstructed conductivity distribution and $\overline{g}$ and $\overline{\hat{g}}$ are the mean values of g and $\hat{g}$ respectively. The image errors and correlation coefficients of the four algorithms are listed in Table Ⅰ and Table Ⅱ, respectively. From Table Ⅰ, for the tested model (a) and (b), the image error derived form APSA method is the smallest. For model (c) and (d), the image error derived form projected SIRT method is the smallest, and the APSA method is a little bigger than it. Result form Table Ⅱ drew the same conclusion, that is, the reconstructed images from APSA algorithm are better comparative with the tested models (a) and (b). For model (c) and (d), the image results are a little worse than those of projected SIRT. The reconstruction results of Fig.2 and Fig.4 are almost the same. Table Ⅰ and Table Ⅱ showed that the image errors and correlation coefficients of these two methods are similar as well.

In order to compare the speed of the four algorithms, the elapsed time was also recorded, see Table Ⅲ. The SIRT and projected SIRT executed longer than the PIOR and APSA method due to that the former two algorithms need a large number of iterations. Although the speed of APSA method is a little lower than PIOR algorithm, since only a few iterative steps are implemented, real-time performance can be ensured. Therefore, there is a trade off between the algorithms execution time and the quality of reconstructed images.
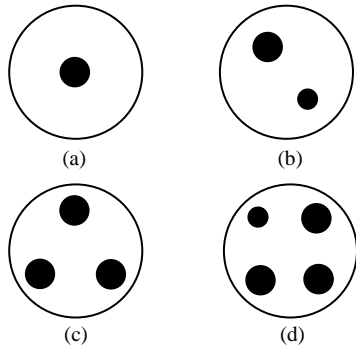

Figure 1.   Tested models

(a) a copper rod of 25mm in diameter

(b) a copper rod of 25mm in diameter and a aluminum rod of 18mm in diameter

(c) three copper rods of 25mm in diameter

(d) three copper rods of 25mm in diameter and a a aluminum rod of 18mm in diameter
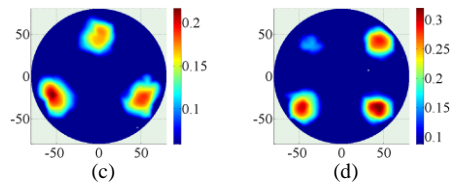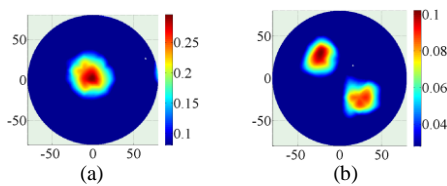

Figure 2.   Reconstructed images using SIRT algorithm
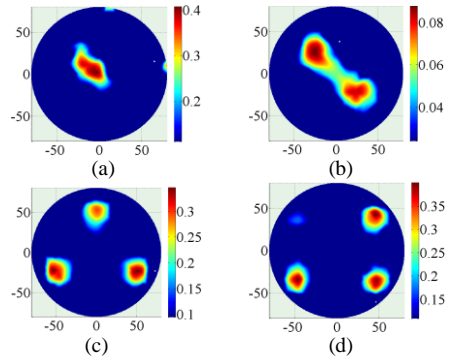

Figure 3.   Reconstructed images using projected SIRT algorithm

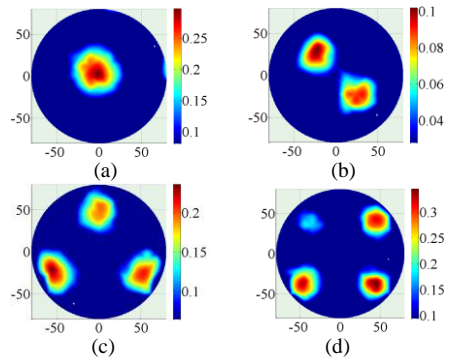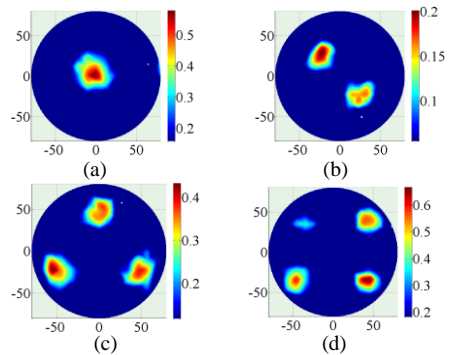Figure 4.   Reconstructed images using PIOR algorithm

Figure 5.   Reconstructed images using PSGI algorithm

TABLE I. IMAGE ERROR (%)

Algorithms and iterations	Reconstructed models			
	(a)	(b)	(c)	(d)
SIRT 1000 iterations	15.59	14.35	14.12	14.31
Projected SIRT 200 iterations	13.91	22.48	9.670	13.00
PIOR 1 iteration	18.04	17.07	18.02	15.35
APSA 5 iterations	12.78	10.22	10.94	14.25

TABLE II. CORRELATION COEFFICIENT

Algorithms and iterations	Reconstructed models			
	(a)	(b)	(c)	(d)
SIRT 1000 iterations	0.6223	0.6657	0.7353	0.7726
Projected SIRT 200 iterations	0.5937	0.5572	0.8446	0.8386
PIOR 1 iteration	0.5819	0.6332	0.7043	0.7520
APSA 5 iterations	0.6759	0.7321	0.7975	0.8114

TABLE III. ELAPSED TIME (MS)

Algorithms and iterations	Reconstructed models			
	(a)	(b)	(c)	(d)
SIRT 1000 iterations	12219	121.88	127.80	128.71
Projected SIRT 200 iterations	36.844	35.128	35.703	28.562
PIOR 1 iteration	0.365	0.281	0.274	0.276
APSA 5 iterations	0.475	0.504	0.481	0.478

V. CONCLUSIONS

In this paper, following the analysis of prior iteration online reconstruction method for SIRT algorithm, an acceleration of projected SIRT reconstructed algorithm was proposed and its formulation was mathematically deduced. This algorithm firstly evaluates the preconditioning matrix using a prior iteration method, then the image is reconstructed via a few iteration steps of projected SIRT algorithm with preconditioning. Reconstructions from measured data confirm that the preconditioning algorithm is effective, the quality of the reconstructed images is relatively high, and the real-time performance is maintained since only a small number of iterative procedures are needed.

REFERENCES

[1] Z. Z. Yu, A. J. Peyton, L. A. Xu, M. S. Beck, "Electromagnetic inductance tomography (EMT): Sensor, electronics and image reconstruction algorithm for a system with a rotatable parallel excitation field," IEE Proceedings- Science, Measurement and Technology, 1998, vol. 145, no. 1, pp. 20-25.

[2] A. J. Peyton, M. S. Beck, A. R. Borges, J. E. Oliveira, G. M. Lyon, Z. Z. Yu, M. W. Brown, J. Ferrerra, "Development of electromagnetic tomography (EMT) for industrial applications. Part 1: Sensor design and instrumentation," 1st World Congress on Industrial Process Tomography, 1999, pp. 306-312.

[3] A. J. Peyton, Z. Z. Yu and G. Lyon, et al., "An overview of electromagnetic inductance tomography: description of three different systems," Measurement Science Technology, 1996, vol. 7, no.3, pp.261-271.

[4] A. V. Korzhenevskii, V. A. Cherepenin, "Magnetic induction tomography," Journal of Communication Technology and Electronics, 1997, vol. 42, no. 4, pp. 469-474.

[5] Y. He, M. He, J. Li, "Review about image reconstruction arithmetic for electromagnetic tomography," Electrical Techniques, 2007, no. 4, pp. 43-48.

[6] L. Y. Li, Z. Liu, Y. Lei, "Simulation analysis of the EMT forward problem and inverse problem," China Science and Technology Information, 2006, no.20, pp.287-290.

[7] W. Yin, A. J. Peyton, "Sensitivity Formulation Including Velocity Effects for electromagnetic Induction Systems", IEEE Transactions on Magnetics, Vol: 46 , no: 5, pp: 1172-1176.

[8] S. Ramli and A. J. Peyton, "Feasibility study of planar-array electromagnetic inductance tomography (EMT)," Proc. 1st World Congress on Industrial Process Tomography, Buxton, 1999, pp. 502-510

[9] H. Griffiths, W. R. Stewart and W. Gough, "Magnetic induction tomography: a measurement system for biological tissues," Ann. NY Acad. Sci., 1999, vol. 873, no. 1, pp. 335-345.

[10] W. Yang, L. Peng, "Image reconstruction algorithms for electrical capacitance tomography," Measurement Science Technology, 2003, vol. 14, no. 1, pp. R1-R13.

[11] S. Liu, W. Yang, H. Wang and F. Jiang, "Prior-online iteration for image reconstruction with electrical capacitance tomography", IEE. Proc.- Sci. Meas. Technol. 2004, vol. 151, no. 3, pp. 195-200.

[12] T.-S. Pan, A. E. Yagle, "Acceleration of Landweber-Type algorithms by syppression of projection on the maximum singular vector," IEEE Transaction On Medical Imaging. 1992, vol. 11, no. 4, pp. 479-487.

[13] W. Yin, G. Chen, L. J. Chen and B. Wang, "The design of a digital magnetic induction tomography (MIT) system for metallic object imaging based on half cycle demodulation," IEEE Sensors Journal, 2011, vol. 11, no. 10, pp. 2233-2240.

[14] N. Terzija, W. Yin, G. Gerbeth, et al., "Electromagnetic inspection of a two-phase flow of GalnSn and argon," Flow Measurement and Instrumenttation, 2011, vol. 22, no. 1, pp. 10-16.

[15] W. Yang, D. M. Spink, T. A. York and H. McCann, "An image-reconstruction algorithm based on Landweber's iteration method for electrical-capacitance tomography," Measurement Science Technology, 1999, vol. 10, pp. 1065-1069.